1997

Effect of Diurnal Convection on Trapped Thermal Plasma in the Outer Plasmasphere

Mark Anthony Reynolds
Embry-Riddle Aeroautical University, reynoldb2@erau.edu

G. Ganguli
National Research Council

J.A. Fedder
George Mason University

D.J. Melendez-Alvira
Naval Research Laboratory

GEOPHYSICAL RESEARCH LETTERS, VOL. 24, NO. 17, PAGES 2255-2258, SEPTEMBER 1, 1997

Effect of diurnal convection on trapped thermal plasma in the outer plasmasphere

M. A. Reynolds,[1] G. Ganguli, and J. A. Fedder[2]
Beam Physics Branch, Plasma Physics Division, Naval Research Laboratory, Washington, D.C.

D. J. Meléndez-Alvira
E. O. Hulburt Center for Space Research, Naval Research Laboratory, Washington, D.C.

Abstract. A kinetic, multi-species model of the plasmasphere is constructed that includes the effect of convection and corotation electric fields on trapped particles in drifting flux tubes. The resulting morphology of the outer plasmasphere is significantly different from the morphology obtained using the assumption of diffusive equilibrium. The difference is due primarily to the contraction and expansion of the region of velocity space accessible to the trapped particles, and has implications for the interpretation of remote sensing experiments.

Introduction

The effects of magnetospheric convection, and its associated large-scale electric field, on the global structure and morphology of the magnetosphere are well known [*Axford,* 1969]. The most striking example in the inner magnetosphere is the formation of the plasmapause, whose location is determined by the interplay between the large-scale electric field and the corotation electric field [*Nishida,* 1966; *Lemaire,* 1974]. The effects of convection on the detailed structure of the region inside the plasmapause are less well known.

Recent work on plasmaspheric convection has utilized fluid methods [*Rasmussen and Schunk,* 1990; *Rasmussen et al.,* 1993; *Khazanov et al.,* 1994], which treat the entire distribution of particles identically. This is reasonable if one assumes that the flux tubes are completely filled, that is, a diffusive equilibrium condition exists. However, convection (the diurnal motion of a magnetic flux tube) affects different regions of the plasma velocity space in fundamentally different ways, leading to a steady state in the high-altitude regions near the plasmapause, but not hydrodynamic or thermal equilibrium. Because this partition in velocity space is not realizable in a fluid formulation, it is necessary to treat the plasma from a kinetic point of view, particularly at high altitudes where Coulomb collisions are infrequent. In addition, the observed density and temperature structure at high altitudes [*Moldwin et al.,* 1995] is difficult to understand from a fluid point of view. The effect of convection on these large-L flux tubes is expected to be strong [*Rasmussen and Schunk,* 1990; *Elphic et al.,* 1997], and differences between measured densities and fluid model predictions have been previously reported [*Rasmussen and Schunk,* 1990; *Craven et al.,* 1997].

In view of these considerations, we use collisionless kinetic theory to investigate the convection of magnetically trapped thermal particles, and to elucidate their role in determining the density and temperature morphology inside the plasmapause. This trapped population, found in high-altitude flux tubes, is thermodynamically isolated from the ionospheric plasma on transport time scales, and is affected by the convection electric fields that form the plasmapause. These flux tubes experience expansion and contraction due to radial excursions during their diurnal trajectory. This affects the velocity- and configuration-space density of the trapped population. Flux-tube motion does not, however, modify the untrapped population because those particles escape and reenter the ionosphere on a time scale ($\sim$ 1 hour) [*Lemaire,* 1989] shorter than that of convection ($\sim$ 12 hours).

In addition, the present approach has the potential for investigating a wide variety of instabilities (due to the nonequilibrium nature of the distribution function) with a possibility of explaining the observed asymmetric wave activity in the outer plasmasphere [*Boardsen et al.,* 1995]. The waves could provide a mechanism for scattering particles between the trapped population and the untrapped population. These velocity-space diffusion effects are not, however, included in the present analysis.

Convection model

We divide the plasmasphere into two regions: the barosphere, where Coulomb collisions dominate and the plasma distribution function is Maxwellian; and the region above the barosphere, which is taken to be collisionless, and where the convection of trapped particles is included. The boundary between these two regions is the baropause, approximated by an infinitesimally thin surface. Beyond the plasmapause, the trapped particles are absent because they are continually convected away toward the magnetopause.

For this study, we consider the low-energy limit, ignoring both curvature and gradient drifts: all particle motion is field aligned, with both energy and magnetic moment conserved. In this limit, there are four classes of particles possible in a closed-field-line region, and they can be identified by their position in velocity space [*Lemaire and Scherer,* 1970]: (1) escaping particles that have small pitch angles, enough energy to escape the gravitational trap, and can enter the other hemisphere, (2) incoming particles that escape from one hemisphere and enter the other, (3) ballistic particles that do not have enough energy to overcome gravity and return to the ionosphere, and (4) trapped particles that are reflected between two mirror points and never encounter

[1]National Research Council – NRL Research Associate.
[2]George Mason University, Fairfax, VA.

Paper number 97GL02021.
0094-8534/97/97GL-02021$05.00

the baropause. The first three classes are in contact with the ionosphere and together make up the portion of the distribution called the source cone. Because of this thermal contact, the characteristics of the source-cone particles, such as temperature and density, are determined by ionospheric conditions. The fourth class (trapped particles) forms a loss cone in velocity space, and can exhibit a morphology different from the ionospherically generated source cone, even during magnetically quiet times.

The velocity distribution is assumed to be Maxwellian at the baropause, transforms into a source-cone distribution as it flows up the field line, and re-enters the barosphere. The trapped particles in each flux tube, however, remain in the flux tube indefinitely (in the limit of no diffusion), and convect under the influence of the combined convection and corotation electric fields. Only those trapped particles that never encounter the baropause during their diurnal motion (and hence would be absorbed) are included. Also, only those trapped particles that drift entirely around the Earth are included. The distribution of the trapped particles is taken to be Maxwellian over the permitted region of velocity space, and their density, relative to that of the source cone, is a free parameter. We do not, however, specify a mechanism for filling the loss cone.

To determine the source-cone distribution quantitatively, the lower boundary condition of a given field line is a normalized, isotropic Maxwellian distribution f_0 (at the baropause) for each species with mass m

$$f_0(\mathbf{v}_0) = n_0 \left(\frac{m}{2\pi k T_0}\right)^{3/2} \exp\left\{-\frac{m\left(v_{\parallel 0}^2 + v_{\perp 0}^2\right)}{2kT_0}\right\}, \tag{1}$$

where n_0, T_0, and $\mathbf{v}_0$ are the baropause density, temperature, and velocity. The source-cone distribution f_s at a higher altitude $\mathbf{r}$ on the same field line is determined by applying Liouville's theorem (conserving energy and magnetic moment) and taking into account the accessibility condition

$$f_s(\mathbf{v},\mathbf{r}) = f_0(\mathbf{v}_0) \times \Theta\left(\frac{B}{B_0 - B}\left[v_\parallel^2 + 2\frac{U - U_0}{m}\right] - v_\perp^2\right), \tag{2}$$

where Θ is the unit step function, B and U are the magnetic field and the potential energy at $\mathbf{r}$, B_0 and U_0 are those quantities at the baropause, and $\mathbf{v}_0(\mathbf{v})$ is the velocity transformation (see, e.g., *Eviatar et al.* [1964]). The potential energy U consists of the gravitational, electrostatic and centrifugal potential energies. The Θ function in Eq. (2) indicates the region of velocity space that the source cone occupies. The density of the source-cone population is determined by integrating the distribution function, $n_s = \int d^3v f_s$, and one obtains

$$n_s(\mathbf{r}) = n_0\left(e^{-\psi} - \sqrt{A}\, e^{-\psi/A}\right), \tag{3}$$

where $\psi = (U - U_0)/kT_0$ is the dimensionless potential energy and $A = 1 - B/B_0$. This result is equivalent to that obtained by *Eviatar et al.* [1964]. The first term in Eq. (3) corresponds to isothermal diffusive equilibrium, while the trapped particles are subtracted by the second term.

To determine the trapped distribution quantitatively, we include the effects of convection on the region of velocity space left undetermined by Eq. (2). We assume that the distribution in this region is proportional to f_0, but that accessibility limits the trapped distribution f_t to

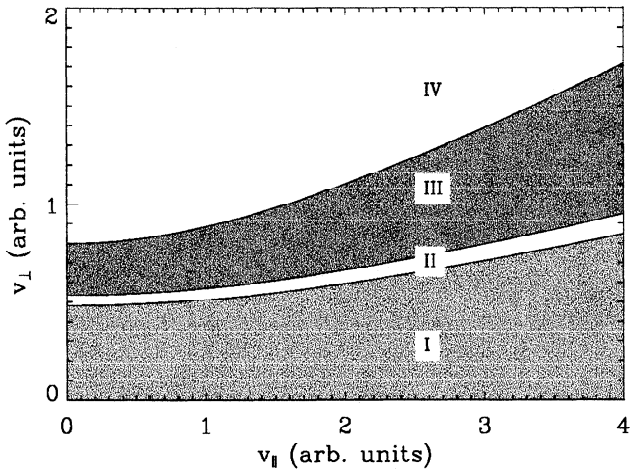

Figure 1. Velocity space at the equator of a typical flux tube. Region I is the source cone, and region III is the trapped population. Particles in region II encounter the baropause, and region IV is not accessible from dawn due to convection. The three boundaries between the regions are determined quantitatively by the three Θ functions in Eqs. (2) and (4).

$$f_t(\mathbf{v},\mathbf{r}) = \eta\, f_0(\mathbf{v}_0) \times \Theta\left(v_\perp^2 - \frac{B}{B_{0d} - B}\left[v_\parallel^2 + 2\frac{U - U_{0d}}{m}\right]\right) \times \Theta\left(\frac{B}{B_d - B}\left[v_\parallel^2 + 2\frac{U - U_d}{m}\right] - v_\perp^2\right), \tag{4}$$

where η is a free parameter that characterizes the density of the trapped population relative to the source cone, B_d and U_d are the magnetic field and potential energy at the equator of the flux tube at its closest to Earth (which we take to be at dawn—this is true for a symmetric electric field), and B_{0d} and U_{0d} are the same quantities at the baropause of the dawn flux tube. Those parameters with a subscript d are controlled by the electric field model, which determines the drift path of the flux tube. The parameter η will depend on flux-tube filling and loss processes, as well as the recent history of the plasmasphere. The first Θ function in Eq. (4) allows only those particles that do not encounter the baropause during their diurnal convection. That is, we keep only those trapped particles whose turning point is always above the baropause. The second Θ function in Eq. (4) is the accessibility condition from dawn for convective motion. That is, we keep only those particles that actually drift completely around the Earth. Equation (4) is the distribution only in the equatorial plane; a similar expression holds at higher latitudes. Integrating over the distribution, the density of the drifting trapped particles, n_t, is

$$n_t(\mathbf{r}) = \eta\, n_0\left(\sqrt{A_{0d}}\, e^{-\psi/A_{0d}} - \sqrt{A_d}\, e^{-\psi - (\psi_d/\beta)}\right), \tag{5}$$

where $A_{0d} = 1 - B/B_{0d}$, $A_d = 1 - B/B_d$, $\psi_d = (U - U_d)/kT_0$, and $\beta = A_d/(1 - A_d)$. Figure 1 shows the regions of velocity space that the two distinct populations occupy, at the equator of a typical flux tube.

The total density is the sum of the two populations, $n = n_s + n_t$, as given by Eqs. (3) and (5). In these expressions the electrostatic potential is undetermined and must be calculated self-consistently by applying the quasineutrality condition

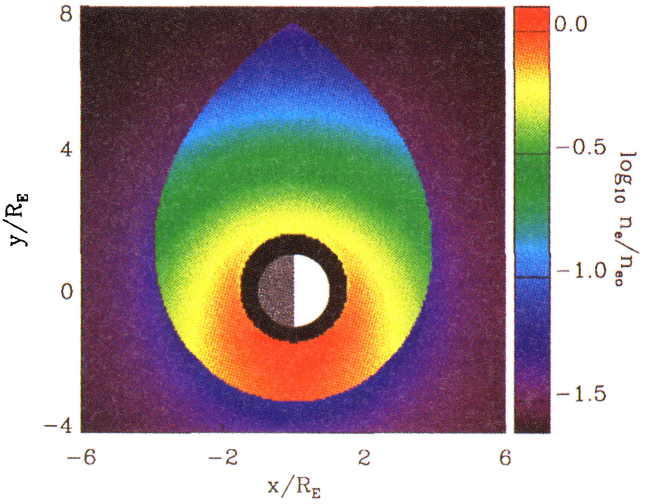

Figure 2. Electron density n_e in the equatorial plane, scaled to the electron density at the baropause, n_{eo}, using the GSM coordinate system. The parameters are $\eta = 1.75$, $r_0 = 3000$ km, $T_0 = 3000$ K, 90% hydrogen and 10% helium at the baropause, and a dawn-dusk electric field of 0.25 mV/m.

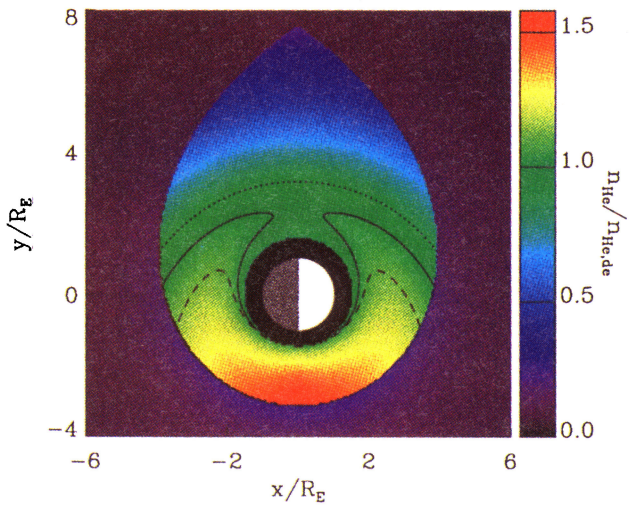

Figure 4. Ratio of helium ion density n_{He} to diffusive equilibrium helium ion density $n_{He,de}$ in the equatorial plane, for the same parameters as Fig. 2. The solid line indicates the surface on which this ratio is unity. Near the plasmapause, this ratio is $\sim$ 1.5 at dusk and is $\sim$ 0.25 at dawn, a factor of 6 difference. The dashed and dotted lines indicate the positions of the unity surfaces for the cases where $\eta = 1.5$ and $\eta = 2.0$, respectively. (The densities for these two cases are not shown.)

$n_e = \sum_i n_i$. The electrons are treated in the same manner as the ions, with $T_e = T_i$.

Besides the density, knowledge of the total distribution allows the calculation of the effective temperature. The distribution functions calculated above exhibit highly anisotropic temperatures, which could lead to strong instabilities. The actual spatial regions of instability will depend on the the parameter η, as well as the specific electric field model.

Equatorial densities

To illustrate the result of treating the trapped particles in the manner described, we now calculate plasma densities in the equatorial plane using the plasmapause formation mechanism of *Nishida* [1966] (corotation and convection electric fields combine to form a separatrix), a uniform dawn-dusk electric field [*Kavanagh et al.*, 1968], a dipolar magnetic field aligned with the rotation axis, a baropause of constant altitude, density and temperature, with only the gravitational and electrostatic potential energies included in U (no centrifugal potential). These simplifications allow us to focus on the contribution of the trapped population, and they can easily be relaxed. For illustrative purposes, we choose two ion species, 90% hydrogen and 10% helium at the baropause, along with $r_0 = 3000$ km, $T_0 = 3000$ K, and a dawn-dusk electric field of 0.25 mV/m.

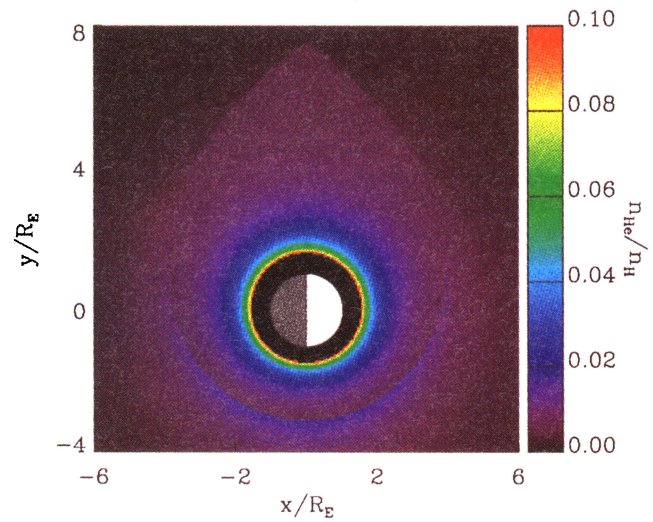

Figure 3. Ratio of helium ion density n_{He} to hydrogen ion density n_H in the equatorial plane, for the same parameters as Fig. 2.

Figure 2 shows the electron density in the equatorial plane for $\eta = 1.75$. Inside the plasmapause (shown with the characteristic teardrop shape expected from the electric field model), the density enhancement in the dawn sector and the density depletion in the dusk sector are due primarily to the convection of the trapped population. The asymmetry is strongest at high altitudes, where convection plays the most important role. Although not shown, the temperature exhibits a similar asymmetry. Outside the plasmapause the density is low because only source-cone particles are present.

Because of the importance of future helium imaging to our understanding of the plasmasphere, Fig. 3 shows the ratio of helium ion density to hydrogen ion density in the equatorial plane. This ratio varies rapidly for $r \lesssim 2R_E$, but varies slowly for $r \gtrsim 2R_E$, in reasonable agreement with statistical studies [*Craven et al.*, 1997]. This behavior is due to the mass ratio of the two species and the interplay between the gravitational and electrostatic potentials. Figure 3 also shows that this ratio is approximately constant across the plasmapause, an observation noted previously [*Horwitz et al.*, 1986].

In order to assess the capability of imaging to distinguish between models, Fig. 4 shows the ratio of the helium ion density given by the present model to what the helium ion density would be if diffusive equilibrium conditions existed. The solid line indicates the surface where the ratio is unity. Dawnward of this surface, the loss cone is overfilled relative to the source cone; duskward of this surface (and outside the plasmapause), the loss cone is underfilled. The dawn-

dusk asymmetry of this ratio affirms the distinguishability of the present model. To illustrate the effect of varying η, the dashed and dotted lines in Fig. 4 indicate the positions of the unity surfaces for the cases where $\eta = 1.5$ and $\eta = 2.0$, respectively. (The densities for these two cases are not shown, but they exhibit an asymmetry as well.)

The present method is not limited to a particular electric field specification or plasmapause formation mechanism; other electric field models [e.g., *Volland,* 1973] or plasmapause models [e.g., *Lemaire,* 1974] can be used. In addition, it is possible to incorporate the effects of the penetration of the polar convection electric field to low latitudes [*Spiro et al.,* 1988; *Doe et al.,* 1992].

Conclusion

We have shown that including trapped particles that drift along diurnal convection equipotentials and adjust their density self-consistently leads to a morphology of the outer plasmasphere that is different from the morphology obtained using the assumption of diffusive equilibrium. The density and temperature exhibit an asymmetry between the dawn and dusk sectors. The partition in velocity space between trapped particles and untrapped particles, and the different effects of convection on the different classes of particles, requires a kinetic theory.

Dynamical effects can be important, especially near the dusk-side bulge. In order to understand the dynamics of this high-altitude region, however, the equilibrium structure, as calculated by the present model, must first be elucidated. Future work will include velocity-space diffusion, higher-order adiabatic invariants, and latitude-dependent baropause models.

Future spacecraft missions will have the capability to globally image the inner magnetosphere (for example, through scattering of the solar 30.4 nm line by He^+), and provide progress in our understanding of the physical processes in the plasmasphere [*Meier,* 1991; *Williams et al.,* 1992]. The present model has a predictive capability [*Reynolds et al.,* 1997] needed to extract quantitative information from the observational data.

Acknowledgments. We would like to acknowledge fruitful discussions with R. R. Meier, J. M. Picone, A. C. Nicholas, and E. C. Roelof. This work is sponsored by the Office of Naval Research and NASA.

References

Axford, W. I., Magnetospheric convection, *Rev. Geophys., 7,* 421, 1969.

Boardsen, S. A., *et al.,* Plasma wave imaging of the Earth's magnetosphere, *Eos Trans. AGU, 76*(46), Fall Meet. Suppl., F521, 1995.

Craven, P. D., D. L. Gallagher, and R. H. Comfort, Relative concentration of He^+ in the inner magnetosphere as observed by the DE 1 retarding ion mass spectrometer, *J. Geophys. Res., 102,* 2279, 1997.

Doe, R. A., M. B. Moldwin, and M. Mendillo, Plasmapause morphology determined from an empirical ionospheric convection model, *J. Geophys. Res., 97,* 1151, 1992.

Elphic, R. C., M. F. Thomsen and J. E. Borovsky, The fate of the outer plasmasphere, *Geophys. Res. Lett., 24,* 365, 1997.

Eviatar, A., A. M. Lenchek, and S. F. Singer, Distribution of density in an ion-exosphere of a nonrotating planet, *Phys. Fluids, 7,* 1775, 1964.

Horwitz, J. L., *et al.,* Dual-spacecraft measurements of plasmasphere-ionosphere coupling, *J. Geophys. Res., 91,* 11,203, 1986.

Kavanagh, L. D., Jr., *et al.,* Plasma flow in the magnetosphere, *J. Geophys. Res., 73,* 5511, 1968.

Khazanov, G. V., *et al.,* Effect of magnetospheric convection on thermal plasma in the inner magnetosphere, *J. Geophys. Res., 99,* 5923, 1994.

Lemaire, J., The 'Roche-limit' of ionospheric plasma and the formation of the plasmapause, *Planet. Space Sci., 22,* 757, 1974.

Lemaire, J., Plasma distribution models in a rotating magnetic dipole and refilling of plasmaspheric flux tubes, *Phys. Fluids B, 1,* 1519, 1989.

Lemaire, J., and M. Scherer, Model of the polar ion-exosphere, *Planet. Space Sci., 18,* 103, 1970.

Meier, R. R., Ultraviolet spectroscopy and remote sensing of the upper atmosphere, *Space Sci. Rev., 58,* 1, 1991.

Moldwin, M. B., *et al.,* The fine-scale structure of the outer plasmasphere, *J. Geophys. Res., 100,* 8021, 1995.

Nishida, A., Formation of plasmapause, or magnetospheric plasma knee, by the combined action of magnetospheric convection and plasma escape from the tail, *J. Geophys. Res., 71,* 5669, 1966.

Rasmussen, C. E., and R. W. Schunk, A three-dimensional time-dependent model of the plasmasphere, *J. Geophys. Res., 95,* 6133, 1990.

Rasmussen, C. E., S. M. Guiter, and S. G. Thomas, A two-dimensional model of the plasmasphere: refilling time constants, *Planet. Space Sci., 41,* 35, 1993.

Reynolds, M. A., *et al.,* Global images of plasmaspheric helium, *Eos Trans. AGU, 78*(17), Spring Meet. Suppl., S278, 1997.

Spiro, R. W., R. A. Wolf, and B. G. Fejer, Penetration of high-latitude-electric-field effects to low latitudes during SUNDIAL 1984, *Ann. Geophys., 6,* 39, 1988.

Volland, H., A semiempirical model of large-scale magnetospheric electric fields, *J. Geophys. Res., 78,* 171, 1973.

Williams, D. J., E. C. Roelof, and D. G. Mitchell, Global magnetospheric imaging, *Rev. Geophys., 30,* 183, 1992.

J. A. Fedder, G. Ganguli, and M. A. Reynolds, Code 6794, Naval Research Laboratory, 4555 Overlook Avenue SW, Washington, DC 20375. (e-mail: anthony@ppdu.nrl.navy.mil)

D. J. Meléndez-Alvira, Code 7643.1, Naval Research Laboratory, 4555 Overlook Avenue SW, Washington, DC 20375.

(Received March 4, 1997; revised June 5, 1997;
accepted June 24, 1997.)